Computer Assisted Mechanics and Engineering Sciences, 7: 707–716, 2000.

An efficient 3D curved beam finite element

Jerzy Rakowski and Przemysław Litewka
Institute of Structural Engineering, Poznań University of Technology
ul. Piotrowo 5, 60-965 Poznań, Poland

(Received November 3, 1999)

The purpose of this paper is to create an efficient finite element for the static analysis of 3D arch structures. It is the circural in-plane element with possibility of out-of-plane action. In the element the influences of shear and axial forces on arch displacements are taken into account. The base is the set of exact shape functions, which fulfil the differential equilibrium equation of 3D arch. These shape functions allow us to obtain the exact element stiffness matrix. The element was tested in several numerical examples, results were compared with available analytical solutions and other numerical results. A very good agreement of the results was obtained.

1. Introduction

The present paper is a continuation of authors' previous research presented in [2] and [3]. It is an expansion of our considerations for the case of 3D loading acting on the plane, curved structures. It is still a case that much effort and space in the literature is devoted to the search of effective finite elements, free of parasitic shear and membrane locking effects. The detailed analysis of current bibliography dealing with it can be found in [3].

In [1] the attempt to create the 3D curved beam element with polynomial shape functions is made. In the present paper the authors introduce to that problem the concept of so called physical shape functions. The feature of these functions is that they contain the parameters describing the physical and geometrical properties of the element. A very general case is considered because the stiffness matrix yielding from these functions contains all the influences resulting from 3D characteristics of the element. Besides the dominating effects of bending and torsional moments, the membrane and both shear effects are taken into account. Despite the complicated form of the shape functions, which exactly fulfil the differential equation of the deformed arch axis corresponding to the considered element, the form of the resulting stiffness matrix is very simple.

The use of this matrix in the calculations eliminates completely the shear and membrane locking effects. The numerical results converge very well to the exact solutions even for a very coarse element mesh. The authors strongly hope that the presented approach can be successfully used to formulate new type of effective shell elements.

The paper consists of four sections. The basic one is Section 2 containing the derived statically exact shape functions as well as the element stiffness matrix. Section 3 presents the results of numerical examples. The concluding remarks are included in Section 4. At the end the bibliography is given.

2. 3D arch finite element

2.1. Introduction

We consider a 2-node, 12-degree-of-freedom element with constant radius of curvature R presented in Fig. 1. The following notation is used:

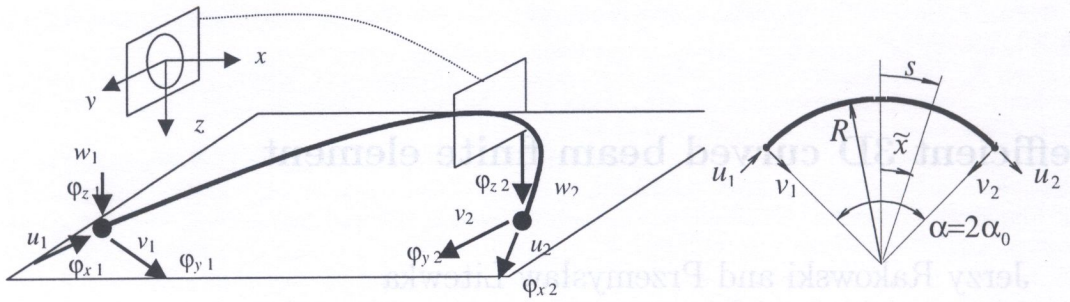

Fig. 1. The 3D arch finite element

i. α is the angle of the element ($\alpha = 2\alpha_0$) and a its lenght ($a = R\alpha$),

ii. $\tilde{x}$ is the angular co-ordinate of element cross-section ($-\alpha_0 \leq \tilde{x} \leq \alpha_0$),

iii. s is curvilinear co-ordinate ($-a/2 \leq s \leq a/2$).

The vector of generalized displacements has a form

$$\begin{aligned}\mathbf{q}^{\mathrm{T}} &= \{q_1\,,\, q_2\,,\, q_3\,,\, q_4\,,\, q_5\,,\, q_6\,,\, q_7\,,\, q_8\,,\, q_9\,,\, q_{10}\,,\, q_{11}\,,\, q_{12}\}^{\mathrm{T}} \\ &= \{u_1\,,\, v_1\,,\, \phi_{z1}\,,\, u_2\,,\, v_2\,,\, \phi_{z2}\,,\, w_1\,,\, \phi_{x1}\,,\, \phi_{y1}\,,\, w_2\,,\, \phi_{x2}\,,\, \phi_{y2}\}^{\mathrm{T}}\end{aligned} \tag{1}$$

where: $\phi_{ki} = a\,\varphi_{ki}$, $k = x, y, z$; $i = 1, 2$, u_i are the nodal tangential displacements, v_i – the radial ones, w_i – the out-of-plane displacements, φ_{zi} – the total rotations of cross-section about z-axis, φ_{yi} – the total rotations of cross-section about y-axis and φ_{xi} – the angles of cross-section twist (i=1,2). The following static equilibrium condition for the element is valid,

$$\mathbf{K} \cdot \mathbf{q} = \mathbf{F}\,, \tag{2}$$

where $\mathbf{K}$ is the element stiffness matrix, $\mathbf{F}$ is a vector of generalized nodal forces corresponding to (1),

$$\mathbf{F}^{\mathrm{T}} = \{H_1\,,\, T_{y1}\,,\, m_{z1}\,,\, H_2\,,\, T_{y2}\,,\, m_{z2}\,,\, T_{z1}\,,\, m_{x1}\,,\, m_{y1}\,,\, T_{z2}\,,\, m_{x2}\,,\, m_{y2}\}^{T}, \qquad m_{ki} = M_{ki}/a\,, \tag{3}$$

H_i are the axial forces, T_{yi} and T_{zi} the shear forces in y and z directions, M_{zi} and M_{yi} the bending moments acting in (x, y) and (x, z) planes, respectively and M_{xi} are the torques.

We consider the element with constant cross-section having the following geometrical properties: I_z, I_y – the second moment of area with respect to z and y-axes, I_s – torsional moment of area, A – area of the cross-section. In order to recognize the influence of internal forces on displacements the dimensionless parameters are introduces where d_z, d_y characterize the shear effects in both directions, e – the membrane effect, t – the torsional effect and b – flexural effect in the second plane. They have the following form:

$$d_y = \frac{EI_z}{\kappa_y GA} \cdot \frac{1}{R^2}\,, \qquad d_z = \frac{EI_z}{\kappa_z GA} \cdot \frac{1}{R^2}\,, \qquad e = \frac{EI_z}{EA} \cdot \frac{1}{R^2}\,, \qquad t = \frac{EI_z}{GI_s}\,, \qquad b = \frac{EI_z}{EI_y}\,, \tag{4}$$

where E and G are Young's and Kirchoff's moduli, κ_y and κ_z are the shear factors in respective directions.

2.2. Element shape functions

In order to find the exact shape functions for the considered arch element we solve in an analytical form the following basic problem.

We determine displacement functions along the s circular axis of the arch element due to unit displacement of its both supports. The element is treated as the 3D circular beam fully clamped

at both ends and it is six times statically indeterminate. Using the flexibility method the unknown forces as well 12 support reactions and all functions of internal forces are determined for all cases of support unit displacements. Then, using the principle of virtual work and reduction theorem, all displacement functions along the 3D circular beam are obtained in which the influence of bending, shear and axial forces are taken into account. In this way the relations between unit tangential, radial, out-of-plane and 3 rotational nodal displacements and the continuous functions of generalized displacements of the arch axis yield the set of 72 exact shape functions.

However the in-plane action represented by the functions of tangential displacements $u(\tilde{x})$, radial displacements $v(\tilde{x})$ and cross-section rotations $\varphi_z(\tilde{x})$ and the out-of-plane action characterized by functions of out-of-plane displacements $w(\tilde{x})$, angle of twist $\varphi_x(\tilde{x})$ and cross-section rotation $\varphi_y(\tilde{x})$ are fully separated. Hence only 36 shape functions are non-zero. Those, corresponding to the in-plane action were given in our earlier papers, e.g. [2] and will not be cited here. They can be taken from there directly provided the notation changes are observed , i.e. e and d in [2] should be replaced by e/α^2 and d_y/α^2, respectively.

The non-zero shape functions corresponding to the out-of plane action are the out-of-plane displacements $w(\tilde{x})$ (shape functions N_{wi}), angles of twist $\varphi_x(\tilde{x})$ (shape functions $N_{\varphi xi}$) and total cross-section rotations $\varphi_y(\tilde{x})$ (shape functions $N_{\varphi yi}$) for the element caused by the nodal displacement $q_i = 1, i = 7, 8, \ldots, 12$. All these functions, like those representing the in-plane action, can be expressed in the trigonometric-algebraic form

$$N_{\delta i}(\tilde{x}) = C_{\delta 0} + C_{\delta 1}\tilde{x} + (C_{\delta 2} + C_{\delta 3}\tilde{x})\sin\tilde{x} + (C_{\delta 4} + C_{\delta 5}\tilde{x})\cos\tilde{x}, \tag{5}$$

where δ refers to w, φ_x and φ_y element displacements and they fulfil the differential equilibrium equation of the continuous arch [5].

The coefficients $C_{\delta j}$ are not numbers but they depend on geometrical and physical properties of the element: α, b, t and d_z . They have the following form:

1. the function of out-of-plane displacements $w(\tilde{x})$ due to $q_7 = w_1 = 1$:

$$N_{w7}(\tilde{x}) = C_{w70} + C_{w71}\tilde{x} + (C_{w72} + C_{w73}\tilde{x})\sin\tilde{x} + (C_{w74} + C_{w75}\tilde{x})\cos\tilde{x}\,, \tag{6}$$

$$C_{w70} = \frac{B_4(\alpha_0 A_3 - s_0 t) - s_0 B_3}{D_3}\,, \qquad C_{w71} = -\frac{B_4 A_3}{D_3}\,,$$

$$C_{w72} = \frac{-c_0^2(B_3 + B_4)A_5 + 2[B_3 + (1 + c_0)B_4]t}{2D_3}\,, \qquad C_{w73} = 0,$$

$$C_{w74} = \frac{(B_3 + B_4)(\alpha_0 A_4 + c_0 s_0 A_5) - 2s_0 B_4 t}{2D_3}\,, \qquad C_{w75} = -\frac{(B_3 + B_4)A_4}{2D_3}\,,$$

2. the function of out-of-plane displacements $w(\tilde{x})$ due to $q_8 = \phi_{x1} = 1$:

$$N_{w8}(\tilde{x}) = C_{w80} + C_{w81}\tilde{x} + (C_{w82} + C_{w83}\tilde{x})\sin\tilde{x} + (C_{w84} + C_{w85}\tilde{x})\cos\tilde{x}\,, \tag{7}$$

$$C_{w80} = \frac{-\alpha_0[c_0 B_3 - (1 - c_0)B_4]A_3 + s_0[c_0 B_2 - (1 - 2c_0)B_3 - (1 - c_0)B_4]t}{D_3} + \frac{c_0 s_0 t}{D_4}\,,$$

$$C_{w81} = \frac{[c_0 B_3 - (1 - c_0)B_4]A_3}{D_3}\,, \qquad C_{w83} = -\frac{s_0 A_4}{2D_4}\,,$$

$$C_{w82} = \frac{c_0^2[c_0 B_2 - (1 - 2c_0)B_3 - (1 - c_0)B_4]A_5 + 2[-c_0 B_2 + (1 - 2c_0 - c_0^2)B_3 + (1 - c_0^2)B_4]t}{2D_3}$$

$$+ \frac{s_0(\alpha_0 A_4 - c_0 s_0 A_5)}{2D_4}\,,$$

$$C_{w84} = \frac{[-c_0 B_2 + (1-2c_0)B_3 + (1-c_0)B_4](\alpha_0 A_4 + c_0 s_0 A_5) + 2s_0[c_0 B_3 - (1-c_0 B_4)]t}{2D_3} + \frac{s_0(s_0^2 A_5 - 2t)}{2D_4},$$

$$C_{w85} = \frac{[c_0 B_2 - (1-2c_0)B_3 - (1-c_0)B_4]A_4}{2D_3},$$

3. the function of out-of-plane displacements $w(\tilde{x})$ due to $q_9 = \phi_{y1} = 1$:

$$N_{w9}(\tilde{x}) = C_{w90} + C_{w91}\tilde{x} + (C_{w92} + C_{w93}\tilde{x})\sin\tilde{x} + (C_{w94} + C_{w95}\tilde{x})\cos\tilde{x}, \tag{8}$$

$$C_{w90} = \frac{-\alpha_0 s_0(B_3 + B_4)A_3 + s_0^2(B_2 + 2B_3 + B_4)t}{D_3} - \frac{c_0^2 t}{D_4}, \qquad C_{w93} = \frac{c_0 A_4}{2D_4},$$

$$C_{w91} = \frac{s_0(B_3 + B_4)A_3}{D_3}, \qquad C_{w95} = \frac{s_0(B_2 + 2B_3 + B_4)A_4}{2D_3},$$

$$C_{w92} = \frac{c_0^2 s_0(B_2 + 2B_3 + B_4)A_5 - 2s_0[(B_2 + 2B_3 + B_4) + c_0(B_3 + B_4)]t}{2D_3} - \frac{c_0(\alpha_0 A_4 - c_0 s_0 A_5)}{2D_4},$$

$$C_{w94} = \frac{-s_0(B_2 + 2B_3 + B_4)(\alpha_0 A_4 + c_0 s_0 A_5) + 2s_0^2(B_3 + B_4)t}{2D_3} - \frac{c_0 s_0^2 A_5 - 2c_0 t}{2D_4},$$

4. the function of angles of twist $\varphi_x(\tilde{x})$ due to $q_7 = w_1 = 1$:

$$N_{\phi x7}(\tilde{x}) = C_{\phi x70} + C_{\phi x71}\tilde{x} + (C_{\phi x72} + C_{\phi x73}\tilde{x})\sin\tilde{x} + (C_{\phi x74} + C_{\phi x75}\tilde{x})\cos\tilde{x}, \tag{9}$$

$$C_{\phi x70} = 0, \qquad C_{\phi x71} = 0, \qquad C_{\phi x73} = 0,$$

$$C_{\phi x72} = \frac{c_0^2(B_3 + B_4)A_5 - 2c_0 B_4 t}{2D_3}, \qquad C_{\phi x74} = \frac{-(B_3 + B_4)(\alpha_0 A_4 + c_0 s_0 A_5)2s_0 B_4 t}{2D_3},$$

$$C_{\phi x75} = \frac{(B_3 + B_4)A_4}{2D_3},$$

5. the function of angles of twist $\varphi_x(\tilde{x})$ due to $q_8 = \phi_{x1} = 1$:

$$N_{\phi x8}(\tilde{x}) = C_{\phi x80} + C_{\phi x81}\tilde{x} + (C_{\phi x82} + C_{\phi x83}\tilde{x})\sin\tilde{x} + (C_{\phi x84} + C_{\phi x85}\tilde{x})\cos\tilde{x}, \tag{10}$$

$$C_{\phi x80} = 0, \qquad C_{\phi x81} = 0, \qquad C_{\phi x83} = \frac{s_0 A_4}{2D_4},$$

$$C_{\phi x82} = \frac{2[c_0 B_3 - (1-c_0)B_4]c_0 t - c_0^2[c_0 B_2 - (1-2c_0)B_3 - (1-c_0)B_4]A_5}{2D_3} - \frac{s_0(\alpha_0 A_4 - c_0 s_0 A_5)}{2D_4},$$

$$C_{\phi x84} = \frac{2s_0[-c_0 B_3 + (1-c_0 B_4)]t + [c_0 B_2 - (1-2c_0)B_3 - (1-c_0)B_4](\alpha_0 A_4 + c_0 s_0 A_5)}{2D_3} - \frac{s_0^3 A_5}{2D_4},$$

$$C_{\phi x85} = \frac{[-c_0 B_2 + (1-2c_0)B_3 + (1-c_0)B_4]A_4}{2D_3},$$

6. the function of angles of twist $\varphi_x(\tilde{x})$ due to $q_9 = \phi_{y1} = 1$:

$$N_{\phi x9}(\tilde{x}) = C_{\phi x90} + C_{\phi x91}\tilde{x} + (C_{\phi x92} + C_{\phi x93}\tilde{x})\sin\tilde{x} + (C_{\phi x94} + C_{\phi x95}\tilde{x})\cos\tilde{x}\,, \tag{11}$$

$$C_{\phi x90} = 0, \qquad C_{\phi x91} = 0, \qquad C_{\phi x93} = \frac{c_0 A_4}{2D_4}\,,$$

$$C_{\phi x92} = \frac{-c_0^2 s_0(B_2 + 2B_3 + B_4)A_5 + 2c_0 s_0(B_3 + B_4)t}{2D_3} + \frac{c_0(\alpha_0 A_4 - c_0 s_0 A_5)}{2D_4}\,,$$

$$C_{\phi x94} = \frac{s_0(B_2 + 2B_3 + B_4)(\alpha_0 A_4 + c_0 s_0 A_5) - 2s_0^2(B_3 + B_4)t}{2D_3} + \frac{c_0 s_0^2 A_5}{2D_4}\,,$$

$$C_{\phi x95} = -\frac{s_0(B_2 + 2B_3 + B_4)A_4}{2D_3}\,,$$

7. the function of cross-section rotations $\varphi_y(\tilde{x})$ due to $q_7 = w_1 = 1$:

$$N_{\phi y7}(\tilde{x}) = C_{\phi y70} + C_{\phi y71}\tilde{x} + (C_{\phi y72} + C_{\phi y73}\tilde{x})\sin\tilde{x} + (C_{\phi y74} + C_{\phi y75}\tilde{x})\cos\tilde{x}\,, \tag{12}$$

$$C_{\phi y70} = \frac{B_4 t}{D_3}\,, \qquad C_{\phi y71} = 0, \qquad C_{\phi y75} = 0,$$

$$C_{\phi y72} = \frac{(B_3 + B_4)(\alpha_0 A_4 + c_0 s_0 A_5) - 2s_0 B_4 t}{2D_3}\,,$$

$$C_{\phi y73} = -\frac{(B_3 + B_4)A_4}{2D_3}\,, \qquad C_{\phi y74} = -\frac{s_0^2(B_3 + B_4)A_5 - 2c_0 B_4}{2D_3}\,,$$

8. the function of cross-section rotations $\varphi_y(\tilde{x})$ due to $q_8 = \phi_{x1} = 1$:

$$N_{\phi y8}(\tilde{x}) = C_{\phi y80} + C_{\phi y81}\tilde{x} + (C_{\phi y82} + C_{\phi y83}\tilde{x})\sin\tilde{x} + (C_{\phi y84} + C_{\phi y85}\tilde{x})\cos\tilde{x}\,, \tag{13}$$

$$C_{\phi y80} = \frac{[-c_0 B_3 + (1 - c_0)B_4]t}{D_3}\,, \qquad C_{\phi y81} = 0, \qquad C_{\phi y85} = \frac{s_0 A_4}{2D_3}\,,$$

$$C_{\phi y82} = \frac{2s_0[c_0 B_3 - (1 - c_0)B_4]t + [-c_0 B_2 + (1 - 2c_0)B_3 + (1 - c_0)B_4(\alpha_0 A_4 + c_0 s_0 A_5)]}{2D_3} - \frac{c_0^2 s_0 A_5}{2D_4}\,,$$

$$C_{\phi y83} = \frac{[c_0 B_2 - (1 - 2c_0)B_3 - (1 - c_0)B_4]A_4}{2D_3}\,,$$

$$C_{\phi y84} = \frac{2c_0[c_0 B_3 - (1 - c_0)B_4]t + s_0^2[c_0 B_2 - (1 - 2c_0)B_3 - (1 - c_0)B_4]A_5}{2D_3} - \frac{s_0(\alpha_0 A_4 - c_0 s_0 A_5)}{2D_4}\,,$$

9. the function of cross-section rotations $\varphi_y(\tilde{x})$ due to $q_9 = \phi_{y1} = 1$:

$$N_{\phi y9}(\tilde{x}) = C_{\phi y90} + C_{\phi y91}\tilde{x} + (C_{\phi y92} + C_{\phi y93}\tilde{x})\sin\tilde{x} + (C_{\phi y94} + C_{\phi y95}\tilde{x})\cos\tilde{x}\,, \tag{14}$$

$$C_{\phi y90} = -\frac{s_0(B_3+B_4)t}{D_3}, \qquad C_{\phi y91} = 0, \qquad C_{\phi y95} = -\frac{c_0 A_4}{2D_4},$$

$$C_{\phi y92} = \frac{2s_0^2(B_3+B_4)t - s_0(B_2+2B_3+B_4)(\alpha_0 A_4 + c_0 s_0 A_5)}{2D_3} + \frac{c_0^3 A_5}{2D_4},$$

$$C_{\phi y94} = \frac{2c_0 s_0(B_3+B_4)t + s_0^3(B_2+2B_3+B_4)A_5}{2D_3} + \frac{c_0(\alpha_0 A_4 - c_0 s_0 A_5)}{2D_4},$$

$$C_{\phi y93} = \frac{s_0(B_2+2B_3+B_4)A_4}{2D_3}.$$

In all formulas (6) to (14) the following simplifying notation is used:

$$B_2 = 2d_z\alpha_0 + t(3\alpha_0 - 4s_0 + c_0 s_0) + b(\alpha_0 A_4 - c_0 s_0 A_5),$$

$$B_3 = t(2s_0 - \alpha_0 + c_0 s_0) - b(\alpha_0 - c_0 s_0), \qquad B_4 = t(\alpha_0 + c_0 s_0) + b(\alpha_0 - c_0 s_0),$$

$$D_3 = B_2 B_4 - B_3^2, \qquad D_4 = t(\alpha_0 - c_0 s_0) + b(\alpha_0 + c_0 s_0),$$

$$A_3 = d_z + t, \qquad A_4 = t + b, \qquad A_5 = t - b.$$

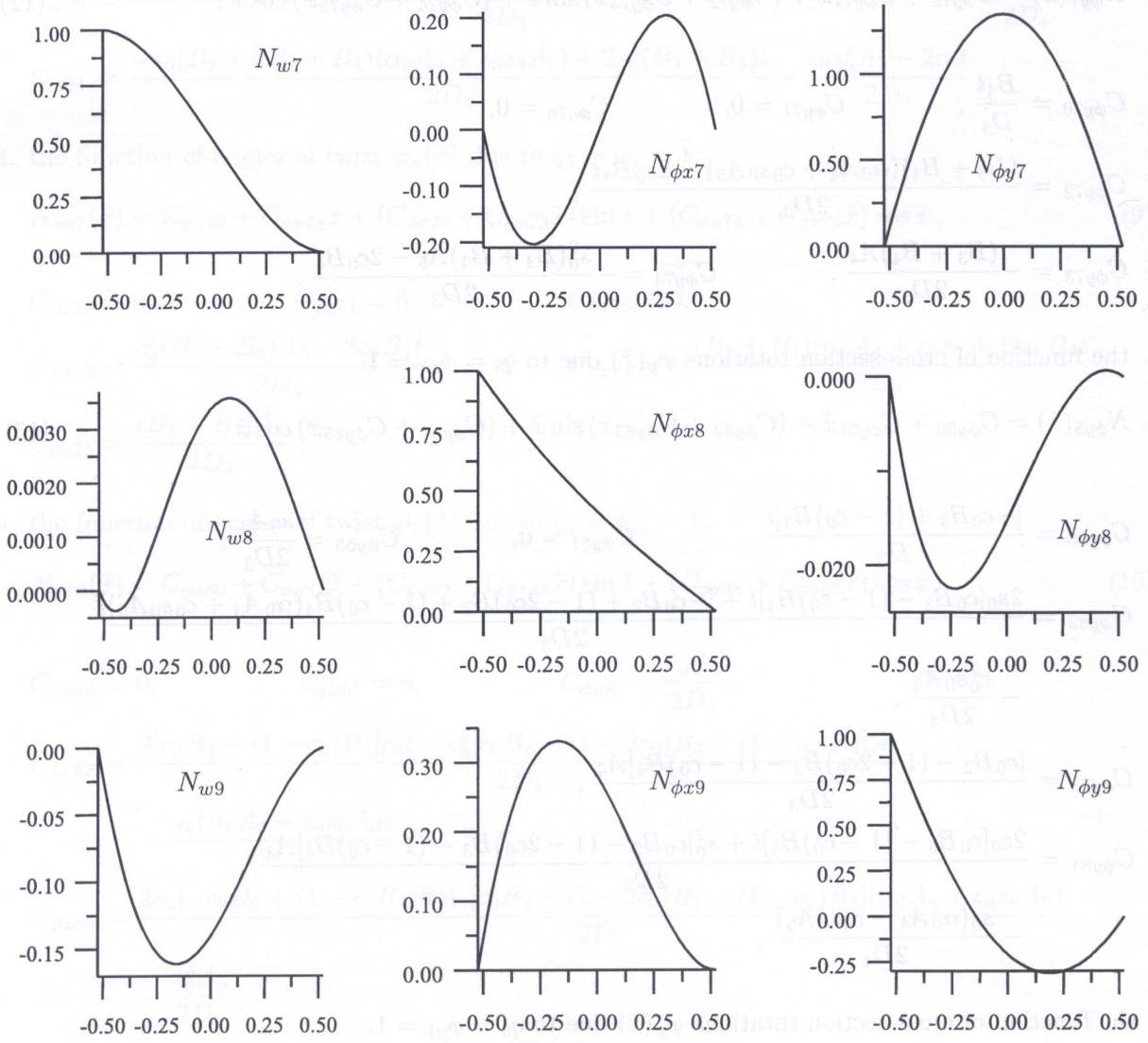

Fig. 2. Graphical representation of element shape functions (data in text)

The shape functions corresponding to the unit nodal displacement of the element node 2 can be obtained from the symmetry and anti-symmetry conditions

$$\begin{aligned}
&N_{w10}(\tilde{x}) = N_{w7}(-\tilde{x}), && N_{w11}(\tilde{x}) = -N_{w8}(-\tilde{x}), && N_{w12}(\tilde{x}) = -N_{w9}(-\tilde{x}),\\
&N_{\phi x10}(\tilde{x}) = -N_{\phi x7}(-\tilde{x}), && N_{\phi x11}(\tilde{x}) = N_{\phi x8}(-\tilde{x}), && N_{\phi x12}(\tilde{x}) = N_{\phi x9}(-\tilde{x}),\\
&N_{\phi y10}(\tilde{x}) = N_{\phi y7}(-\tilde{x}), && N_{\phi y11}(\tilde{x}) = N_{\phi y8}(-\tilde{x}), && N_{\phi y12}(\tilde{x}) = N_{\phi y9}(-\tilde{x}).
\end{aligned}$$

Figure 2 presents the functions graphically for the following data: $r/R = 0.1$; Poisson's ratio $\nu = 0.3$; $\kappa_y = 1.(1)$; $\alpha = \pi/6$.

2.3. Element stiffness matrix

According to standard FEM approach the element stiffness matrix can be obtained from the minimization of the strain energy for the element with respect to nodal generalized displacements. For the case of 3D arch this formula has the following form [1]:

$$\begin{aligned}
U = &\int_s \frac{EI_z}{2}\left(\frac{\partial\varphi_z}{\partial s}\right)^2 \mathrm{d}s + \int_s \frac{GA}{2\kappa_y}\left(\varphi_z - \frac{\partial v}{\partial x} - \frac{u}{R}\right)^2 \mathrm{d}s + \int_s \frac{EA}{2}\left(\frac{\partial u}{\partial s} - \frac{v}{R}\right)^2 \mathrm{d}s\\
&+ \int_s \frac{EI_y}{2}\left(\frac{\partial\varphi_y}{\partial s} + \frac{\varphi_x}{R}\right)^2 \mathrm{d}s + \int_s \frac{GA}{2\kappa_z}\left(\varphi_y + \frac{\partial w}{\partial s}\right)^2 \mathrm{d}s + \int_s \frac{GI_s}{2}\left(\frac{\partial\varphi_x}{\partial s} - \frac{\varphi_y}{R}\right)^2 \mathrm{d}s\,. \qquad (15)
\end{aligned}$$

All functions in (15), i.e. $u(s)$, $v(s)$, $w(s)$, $\varphi_x(s)$, $\varphi_y(s)$, $\varphi_z(s)$, according to the superposition rule, are expressed by the adequate shape functions and all nodal displacements. The first three terms in (15) correspond to the in-plane action while the last three ones characterize the out-of-plane effects. Since the shape functions for those effects are completely independent, the resulting element stiffness matrix is likewise. It can be therefore represented as follows,

$$\mathbf{K} = \frac{EI_z}{R^3} \cdot \begin{bmatrix} \mathbf{K}_{2D(6\times6)} & \mathbf{0} \\ \mathbf{0} & \mathbf{K}_{3D(6\times6)} \end{bmatrix}. \qquad (16)$$

The elements of the stiffness matrix can also be easily obtained from the stiffness matrix definition. If we consider that its each component represents a respective support reaction in the element treated as the clamped-clamped arch, evoked by given unit support displacement, a very simple form of the stiffness matrix can be achieved in a straightforward manner. These support reactions were obtained in the solving procedure of the shape functions (determination of the nodal and internal forces in the arch element caused by unit support displacement using the flexibility method). The resulting submatrix $\mathbf{K}_{2D}$ for in-plane analysis was given in [3]. Here we will present only the new submatrix $\mathbf{K}_{3D}$. It is a symmetric one, $k_{ij} = k_{ji}$ has the following components:

$$\begin{aligned}
k_{7,7} &= \frac{B_4}{D_3}, & k_{7,8} &= \frac{-c_0B_3 + (1-c_0)B_4}{D_3}, & k_{7,9} &= \frac{-s_0(B_3+B_4)}{D_3},\\
k_{7,10} &= -k_{7,7}, & k_{7,11} &= -k_{7,8}, & k_{7,12} &= -k_{7,9},\\
k_{8,8} &= \frac{c_0^2B_2 - 2c_0(1-c_0)B_3 + (1-c_0)^2B_4}{D_3} + s_0^2D_4, & & & &\\
k_{8,9} &= \frac{c_0s_0B_2 - s_0(1-2c_0)B_3 - s_0(1-c_0)^2B_4}{D_3} - c_0s_0D_4, & k_{8,10} &= -k_{7,8}, & &\\
k_{8,11} &= -\frac{c_0^2B_2 - 2c_0(1-c_0)B_3 + (1-c_0)^2B_4}{D_3} + \frac{s_0^2}{D_4}, & & & &\\
k_{8,12} &= \frac{c_0s_0B_2 - s_0(1-c_0)B_3 - s_0(1-c_0)^2B_4}{D_3} + \frac{c_0s_0}{D_4}, & & & &
\end{aligned} \qquad (17)$$

$$k_{9,9} = \frac{s_0^2(B_2+2B_3+B_4)}{D_3} - \frac{c_0^2}{D_4}, \qquad k_{9,10} = -k_{7,9},$$

$$k_{9,12} = \frac{s_0^2(B_2+2B_3+B_4)}{D_3} - \frac{c_0^2}{D_4}, \qquad k_{9,11} = -k_{8,12},$$

$$k_{10,10} = k_{7,7}, \qquad k_{10,11} = k_{7,8}, \qquad k_{10,12} = -k_{7,9},$$

$$k_{11,11} = k_{8,8}, \qquad k_{11,12} = -k_{8,9}, \qquad k_{12,12} = -k_{9,9}.$$

The comparison the above results with those yielding from the standard, strain energy minimization approach (15) and after tedious mathematical calculations obtained the identity. Yet, it is worthwhile to point out that despite the relatively complicated form of the element shape functions (6) to (14) the resulting element stiffness matrix is quite simple.

3. Numerical examples

Several numerical examples were performed in order to compare the results yielding from the use of the elaborated element with the available analytical and numerical solutions.

Example 1

For the cantilever arch presented in Fig. 3 which is loaded by the out-of-plane force at the tip point B the out-of-plane deflection w_B as well as the bending moment and torque at the support are calculated and compared with well known analytical solutions taken from [1].

In the calculation the following data were used:

cross-section depth:	$h = 1$,	included angle:	$\sum \alpha = \pi/2$,
cross-section width:	$b = 1$,	Young's modulus:	$E = 1 \cdot 10^7$,
point load:	$P = 1$,	Poisson's ratio:	$\nu = 0$.
arch radius:	$R = 1$,		

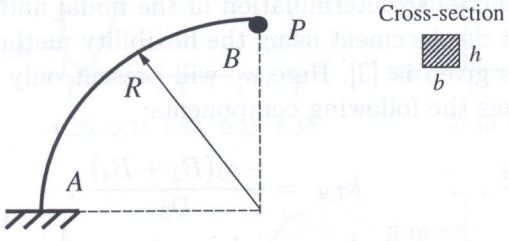

Fig. 3. The arch layout for Example 1

Table 1. Results of Example 1

—	Analytical [1]	Numerical (present)
w_B	0.173	0.173
M_{xA}	5.0	5.0
M_{yA}	5.0	5.0

Example 2

For the clamped-clamped arch shown in Fig. 4, loaded by the out-of-plane force at the centre point, displacements at this point and the bending moments and torques are calculated and compared with the numerical results presented in [4].

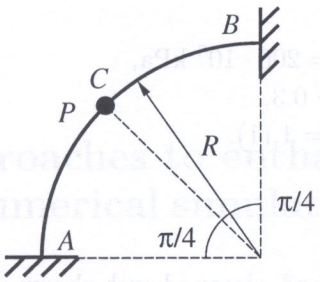

Fig. 4. The arch layout for Example 2

Table 2. Results of Example 2

—	Numerical [4]	Numerical (present)
w_B [m]	0.0098681	0.0100056
φ_{xB} [rad]	0.022500	0.022522
M_{xA} [kNm]	4.86	4.92
M_{yA} [kNm]	32.81	32.75
M_{zB} [kNm]	20.81	20.88

In the calculation the following data were used:

second moment of area (in plane): $I_z = 216 \text{ in}^4 = 8.99 \times 10^{-5} \text{ m}^4$,
second moment of area (out-of-plane): $I_y = 354 \text{ in}^4 = 1.47 \times 10^{-4} \text{ m}^4$,
torsional moment of area: $I_s = 24.5 \text{ in}^4 = 1.02 \times 10^{-5} \text{ m}^4$,
cross section area: $A = 72 \text{ in}^2 = 4.65 \times 10^{-2} \text{ m}^2$,
arch radius: $R = 108 \text{ in} = 2.74 \text{ m}$,
included angle: $\sum \alpha = \pi/2$,
Young's modulus: $E = 4240 \text{ psi} = 29.3 \text{ MPa}$,
Poisson's ratio: $\nu = 0.2045$,
point load: $P = 11 \text{ kips} = 49.0 \text{ kN}$.

In both above examples a very good agreement between present results and available analytical and numerical solutions was obtained. This proves that the elaborated arch element can be succesfully used in the static analysis of 3D arch structures. It should also be emphasized that the discrepancies between our results for Example 2 and those taken from [4] are due to the approximate character of the latter ones. The use of our element for the static analysis of circular arches yields the results coinciding with the exact solutions (see Example 1).

Next examples are aimed at the determining of the influence of the shear forces on the calculated displacements in the case of out-of-plane action. For the similar in-plane analysis refer to [2, 3].

Example 3

For the cantilever arch presented in Fig. 5 loaded by the out-of-plane tip point loadr P the tip deflection is calculated with the varying curvature ratio r/R (r varies) taking into account the shear effect and neglecting it. The comparison of those two sets of results gives the possibility to assess the shear force influence.

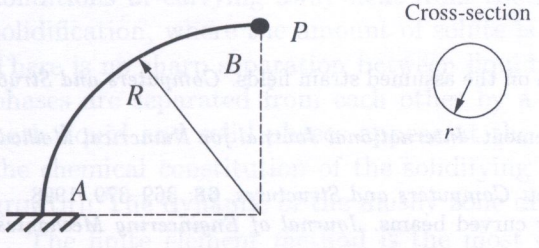

Fig. 5. The arch layout for Example 3

Table 3. Results of Example 3

r/R	w_B [m]	$w_B^{(dz=0)}$ [m]	$w_B^{(dz=0)}/w_B$
0.200	0.51480E−5	0.49674E−5	0.9649
0.100	0.80201E−4	0.79479E−4	0.9910
0.050	0.12745E−2	0.12716E−2	0.9977
0.025	0.20358E−1	0.20346E−1	0.9994
0.010	0.79486E0	0.79479E0	0.9999
0.001	0.79479E4	0.79479E4	1.0000

In the calculation the following data were used:

point load:	$P = 1$ kN,	Young's modulus:	$E = 200 \cdot 10^6$ kPa,
arch radius:	$R = 1$ m,	Poisson's ratio:	$\nu = 0.3$,
included angle:	$\sum \alpha = \pi/2$,	shear factor:	$\kappa_y = 1.(1)$.

Example 4

The similar analysis as in the Example 3 is performed for the clamped–clamped arch shown in Fig. 6 loaded out-of-plane at the centre by point load P. The data remain the same as above, except for included angle: $\sum \alpha = \pi$.

Results of numerical calculations presented in Tables 3 and 4 show that the shear effects is not very important to be taken into account for a very wide range of arch curvature. Only for relatively high ratio of r/R, rather unexpected in the typical civil engineering applications it becomes vital. Hence, the similar conclusion as for the in-plane analysis, see [2] can be made that in practical cases of arch structures the shear effect can safely neglected.

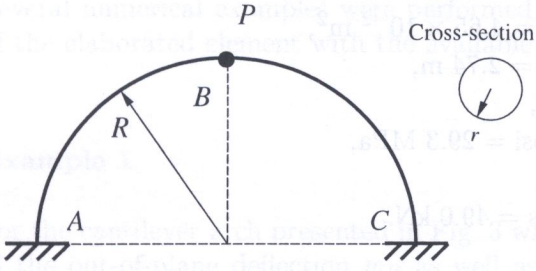

Fig. 6. The arch layout for Example 4

Table 4. Results of Example 4

r/R	w_B [m]	$w_B^{(dz=0)}$ [m]	$w_B^{(dz=0)}/w_B$
0.200	0.11175E−5	0.10272E−5	0.9192
0.100	0.16797E−4	0.16436E−4	0.9785
0.050	0.26440E−2	0.26296E−2	0.9945
0.025	0.42132E−1	0.42075E−1	0.9986
0.010	0.16439E0	0.16436E0	0.9997
0.001	0.16436E4	0.16436E4	1.0000

4. Conclusions

In the present paper the new 3D arch finite element for the static analysis is derived. In the first step the analytical shape functions for the element are determined. It is found out that the in-plane and out-of-plane effects are fully separated.

These functions are then used to obtain a very simple form of element stiffness using standard FEM approach with minimization of 3D arch strain energy with respect to the nodal displacements. The same resulting matrix is obtained from the definition of stiffness matrix components. It must be emphasized that this stiffness matrix in the case of nodal loads provides the exact solution of the static problems independent of the element mesh as it bases on the statically exact shape functions.

These functions can be used to obtain consistent mass matrix and consistent geometrical matrix, which may provide the tool for the calculation of dynamics and stability of 3D arches. Moreover, in our opinion, the elaborated element gives a real possibility to the further development aimed at the analysis of shells of revolution (e.g. domes) using gridwork analogy.

References

[1] J.-K. Choi, J.-K. Lim. General curved beam elements based on the assumed strain fields. *Computers and Structures*, **55**(3): 379–386, 1995.

[2] P. Litewka, J. Rakowski. An efficient curved beam finite element. *International Journal for Numerical Methods in Engineering*, **40**: 2629–2652, 1997.

[3] P. Litewka, J. Rakowski. The exact thick arch finite element. *Computers and Structures*, **68**: 369–379, 1998.

[4] S. J. Pantazopoulou. Low-order interpolation functions for curved beams. *Journal of Engineering Mechanics*, **118**(2): 329–350, 1992.

[5] G. Rakowski, R. Solecki. *Curved Bars. Static Calculations* (in Polish). Arkady, Warszawa, 1966.